Clinical Radiology 68 (2013) e689–e697

Contents lists available at SciVerse ScienceDirect

Clinical Radiology

journal homepage: www.clinicalradiologyonline.net

Pictorial Review

Potential role of advanced MRI techniques for the peritumoural region in differentiating glioblastoma multiforme and solitary metastatic lesions

E.J. Lee [a,*], K.J. Ahn [b], E.K. Lee [c], Y.S. Lee [a], D.B. Kim [a]

[a] Department of Radiology, Dongguk University Ilsan Hospital, Goyang, Republic of Korea
[b] Department of Radiology, Seoul St Mary's Hospital, The Catholic University of Korea, Republic of Korea
[c] Department of Radiology, Seoul National University College of Medicine, Seoul, Republic of Korea

ARTICLE INFORMATION

Article history:
Received 5 March 2013
Received in revised form
10 June 2013
Accepted 14 June 2013

Differentiation between solitary metastatic lesions and glioblastomas, two of the most common malignant brain neoplasms, is often a diagnostic challenge. The purpose of this review is to emphasize the potential roles of advanced magnetic resonance imaging (MRI) techniques, including diffusion-based techniques, such as diffusion-weighted imaging (DWI), exponential DWI, and diffusion tensor imaging, MR perfusion, and MR spectroscopy, as well as conventional MRI, in making a distinction between glioblastomas and solitary metastases in peritumoural regions. Integration of advanced MRI features with conventional MRI, may provide valuable information for differentiating glioblastoma from solitary metastatic lesions.

Introduction

Intracranial metastases and glioblastomas are the two of the most common brain neoplasms in adults. In many clinical settings, especially in patients with multiple lesions, the diagnosis of brain metastasis is usually straightforward and uncomplicated. However, in cases presenting with unknown primary malignancies and solitary intracranial metastatic lesions, differentiation may be difficult.

Conventional magnetic resonance imaging (MRI) has a limited capacity to differentiate these two types of intracerebral lesions, because their neuroimaging appearance is often similar, equivocal, or indistinguishable.[1–6]

In a study that analysed a large variety of morphological criteria and MRI signal characteristics in different sequences,[7] the ratio of the maximum diameter of the peritumoural area to the maximum diameter of the enhancing mass area as measured on T2-weighted images, was the only useful criterion to distinguish between single supratentorial brain metastases and glioblastoma with a lower ratio favouring glioblastoma multiforme (GBM; accuracy 68%, sensitivity 84%, and specificity 45%); the cut-off point for the ratio was calculated to be 2.35.

However, in many cases, a biopsy is performed for histological confirmation, even when there is a history of a known primary malignancy. Discriminating those lesions in the preoperative period is important as treatment approaches vary.[1–6] In patients with glioblastomas, surgical removal followed by external beam irradiation represents a standard treatment. Conversely, patients with suspected brain metastases without a clinical history of systemic cancer should undergo a complicated systemic staging to

* Guarantor and correspondent: E. J. Lee, Department of Radiology, Dongguk University Ilsan Hospital, 814 Siksa-dong, Ilsandong-gu, Goyang-si, Gyeonggi-do 410-773, Republic of Korea. Tel.: +82 31 961 7827; fax: +82 31 961 8281.
E-mail address: ejl1048@hanmail.net (E.J. Lee).

0009-9260/$ – see front matter © 2013 The Royal College of Radiologists. Published by Elsevier Ltd. All rights reserved.
http://dx.doi.org/10.1016/j.crad.2013.06.021

determine the site of the primary carcinoma and evaluate other distant metastases before any surgical intervention or medical therapy. The treatment of brain metastases includes corticosteroids, anticonvulsants, radiotherapy, surgery, radiosurgery, and chemotherapy[8,9].

Most of these tumours are surrounded by a high T2 signal abnormality that, traditionally, has been termed vasogenic oedema. Vasogenic oedema is the most frequent form of brain oedema, which is associated with brain tumours. In general, the non-enhancing area of the abnormality that surrounds the enhancing tumour core is referred to as peritumoural oedema. At histopathological examination, peritumoural signal abnormality represents a tumour-induced increase in interstitial water due to alterations in capillary permeability and the breakdown of the blood–brain barrier. Glioblastoma tend to grow in an infiltrative manner, which typically invades the surrounding tissues, especially white matter tracts, microscopically for several centimetres beyond the area of the enhancing tumour. In glioblastomas, peritumoural areas demonstrate not only altered capillary morphological findings and interstitial water, but also scattered tumour cells infiltrating newly formed or pre-existing, but dilated, vascular channels. Therefore, in glioma, peritumoural oedema is better referred to as infiltrative oedema. Conversely, metastatic tumours tend to grow in an expansile manner, and typically displace the surrounding brain tissues, rather than invade them. In metastatic brain tumours or in non-infiltrative primary tumours, such as meningioma, the peritumoural oedema is synonymous with vasogenic oedema, which increases extracellular water from the leakage of plasma fluid. Therefore, the key to making the distinction between these two entities appears to lie in detecting the changes within the peritumoural area.[1–6,10] Conventional MRI has limited sensitivity and specificity in determining tumour infiltration in the peritumoural area.[11] Advanced MRI techniques are increasingly used to obtain physiological and metabolic information that complements the anatomical images provided by conventional MRI.[3–5] Many new developments in MRI techniques have been used in an effort to make this distinction in the peritumoural area, including diffusion-based techniques, MR perfusion, and MR spectroscopy (MRS). [1–6] This article focuses on the potential roles of advanced MRI techniques, including diffusion-based techniques, such as the absolute diffusion co-efficiency (ADC) measurement, exponential diffusion-weighted imaging (DWI) and diffusion tensor imaging (DTI), perfusion imaging and MRS, as well as conventional MRI, in making a distinction between glioblastomas and solitary metastases in peritumoural regions.

Role of fluid-attenuated inversion recovery or T2-weighted imaging

There is a relatively greater extracellular water content in peritumoural vasogenic oedema associated with metastasis compared with that of glioblastoma, because of the presence of infiltrating neoplastic cells in glioblastoma. Thus, in glioblastoma, a relatively decreased signal area in the peritumoural fluid-attenuated inversion recovery (FLAIR) or T2 hyperintense signal intensity may be expected compared with that of metastasis. Characteristically, metastases involve the subcortical white matter and grey–white matter junction, and have extensive white matter vasogenic oedema. The viable tumour component enhances when intravenous contrast medium is administrated.

Tang et al.[3] suggested that the non-enhancing adjacent cortical signal abnormality detected by FLAIR has the potential to differentiate between gliomas and solitary metastases.[3] Any non-enhancing signal intensity abnormality involving the cortex should represent infiltration of the glial cells. In that study, the authors showed that the presence of a non-enhancing adjacent cortical signal intensity abnormality had a sensitivity of 44% and specificity of 91%, indicating that this signal is specific but not particularly sensitive; the positive predictive value (PPV) for glioma was 84% and the negative predictive value (NPV) was 61%. In a solitary enhancing cerebral lesion, the presence of non-enhancing involvement of the adjacent cortex is a frequent and relatively specific sign for glioblastoma (Figs 1 and 2).[3,10]

Role of DWI: ADC measurement

DWI, which is currently the only MRI technique that provides information on water diffusion, involves the use of phase-defocusing and phase-refocusing gradients to enable the evaluation of the rate of microscopic water diffusion within tissues. DWI has been used to grade or differentiate brain tumours based on cellularity.[12] Because the majority of the translational movement of water occurs in the extracellular space, increased cellularity or swelling should affect the ADC, causing a drop in the values. Several studies have shown that the ADC correlates well with tumour cellularity at histological examination, and calculation of the ADC together with conventional MRI may aid the characterization of cerebral tumours.[12–18]

Several studies in the literature have suggested that the tumoural ADC value is not useful for discriminating metastatic tumours from high-grade gliomas.[11,13,14,18,19] However, Chiang et al.[4] found significantly different tumoural ADC values in malignant gliomas and metastases using 3 T MRI equipment.[4]

Differentiation between metastasis and glioblastoma using signal intensity in the peritumoural region has been attempted with DWI. Brain neoplasms with higher cellularity may show a significant reduction in ADC values, which hypothetically could delineate areas of neoplastic cell infiltration in the peritumoural region[4,13,14]. Several studies have shown the usefulness of the ADC value in the peritumoural region to differentiate glioblastoma and solitary metastasis, and found that the mean or minimum ADC values in peritumoural oedema of metastases are significantly higher than those in high-grade gliomas (Figs 3 and 4).[4,11,14,20,21] Their results support the hypothesis that mean or minimum ADC values can detect neoplastic cell infiltration in the peritumoural region. In a previous study that applied receiver operating characteristic (ROC) curve analysis, a cut-off value

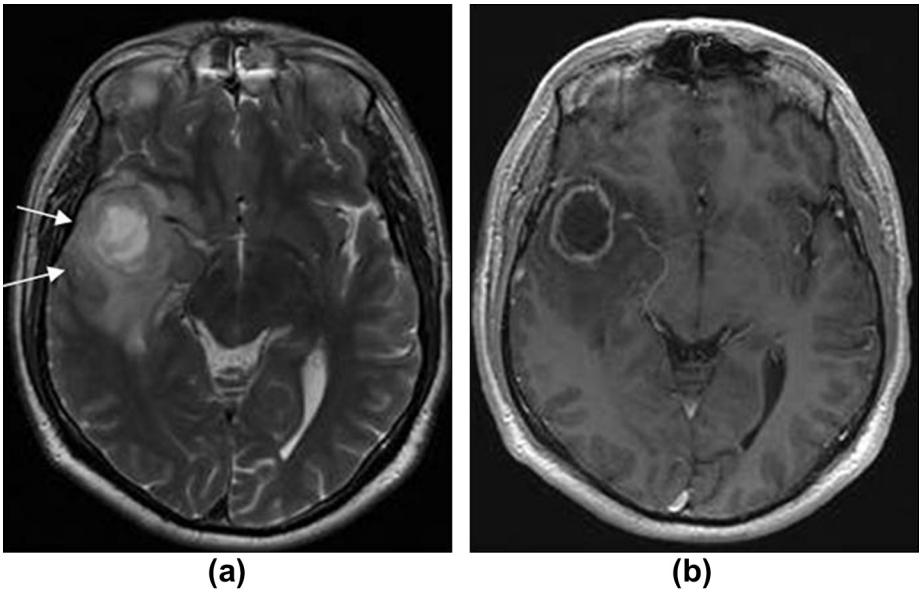

Figure 1 Histologically proven glioblastoma in a 54-year-old man. (a) Axial T2-weighted image and (b) contrast-enhanced T1-weighted image show a peripheral enhancing mass in the right temporal lobe. A cortical T2 hyperintense mass with both the enhancing and non-enhancing components of the lesion is evident. The presence of non-enhancing cortical T2 signal abnormality (arrows), adjacent to the enhancement, implies tumour infiltration.

of 1.302×10^{-3} mm^2/s for the minimum peritumoural ADC value generated the best combination of sensitivity (82.9%) and specificity (78.9%) for distinguishing between glioblastoma and metastasis.[21] The higher ADC value in the peritumoural regions of metastases suggests higher intracellular and extracellular water fractions than in the peritumoural regions of glioblastomas. However, a few studies have shown that DWI is not useful in determining the presence of peritumoural neoplastic cell infiltration.[22,23]

Role of exponential DWI

Signal intensity at DWI is influenced by two factors: water diffusibility and the intrinsic T2 properties of the tissue being examined. The relative contributions of abnormal diffusion and the intrinsic T2 properties are difficult to determine on DWI alone. The resultant hyperintense signal on DWI, which is attributable to the intrinsic T2 signal characteristics, is termed the T2 "shine-through"

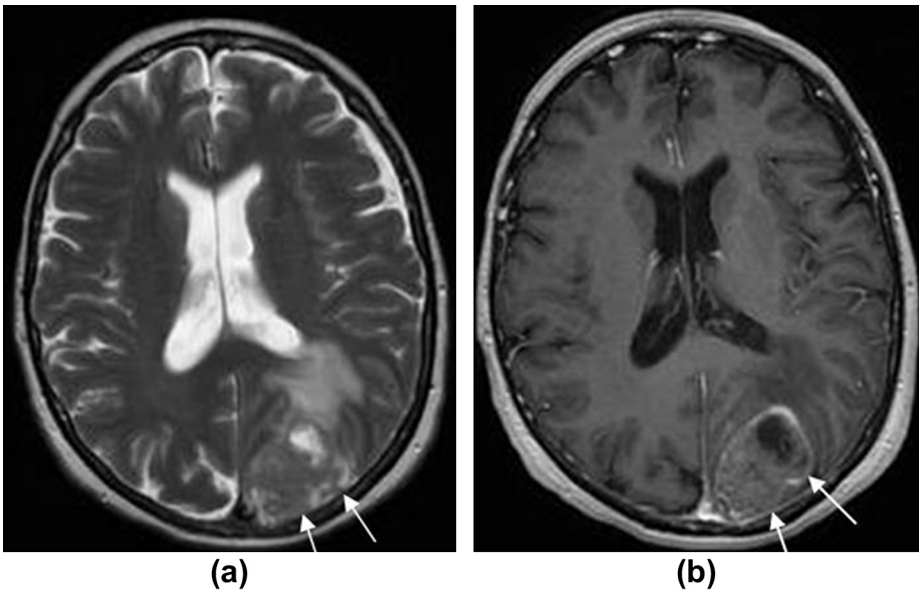

Figure 2 Histologically proven metastasis from anal squamous cell carcinoma in a 77-year-old woman. (a) Axial T2-weighted image and (b) contrast-enhanced T1- weighted image show a heterogeneous enhancing mass in the left occipital lobe. There is cortical T2 signal intensity abnormality related to this lesion, which enhances on the contrast-enhanced T1-weighted image (arrows). Non-enhancing cortical T2 signal intensity abnormality is absent.

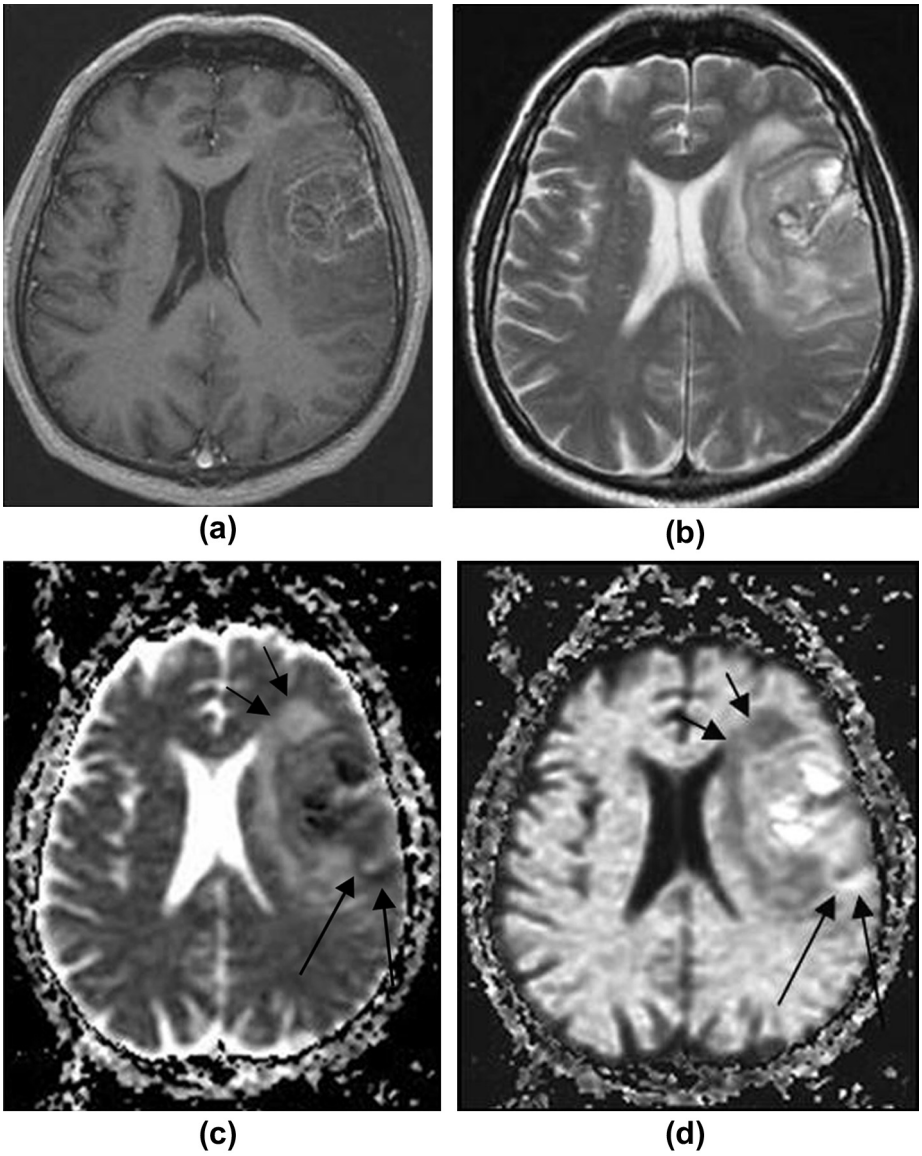

Figure 3 Histologically proven glioblastoma in a 72-year-old man. (a) Contrast-enhanced T1-weighted image and (b) T2-weighted image show a heterogeneous enhancing mass in the left frontal lobe with large peritumoural non-enhancing area. (c) On the ADC map, the enhancing mass has restricted diffusion with small cystic change. The non-enhancing peritumoural region reveals different signal intensities. The intermediate ADC value (long arrows) is thought to represent infiltrative oedema. Increased signal intensity (short arrows) is thought to represent purely vasogenic oedema. (d) Exponential DWI image reveals reverse signal intensity with the ADC map. Presumptive infiltrative oedema (long arrows) shows relatively intermediate signal intensity, and presumptive vasogenic oedema (short arrows) demonstrates markedly decreased signal intensity. Exponential DWI shows visually obvious differentiation between infiltrative oedema and vasogenic oedema.

effect. The exponential image can be generated on a workstation through simple image algebra, and is derived by dividing the maximal B value DWI image, by the B0 image. In mathematical terms, exponential DWI represents the negative exponential of the ADC and can be considered a calculated or synthetic DWI, without T2 shine-through effects. Therefore, exponential DWI provides a more accurate depiction of diffusion effects than trace DWI by removing the contribution from the T2 signal intensity of the tissue being examined.[24,25]

Peritumoural oedema of glioblastoma and metastasis reveals obviously different signal intensities at exponential DWI. Tumour-infiltrative oedema of glioblastoma shows relatively intermediate signal intensity at exponential DWI (Fig 3d), and vasogenic oedema of metastasis demonstrates markedly decreased signal intensity relative to the brain parenchyma (Fig 4c).

Role of DTI

DTI and fibre tractography are more recently developed DWI methods, which can demonstrate the orientation and integrity of white matter fibres *in vivo*. The metrics commonly used include the mean diffusivity (MD) and fractional anisotropy (FA). MD represents a measure of the

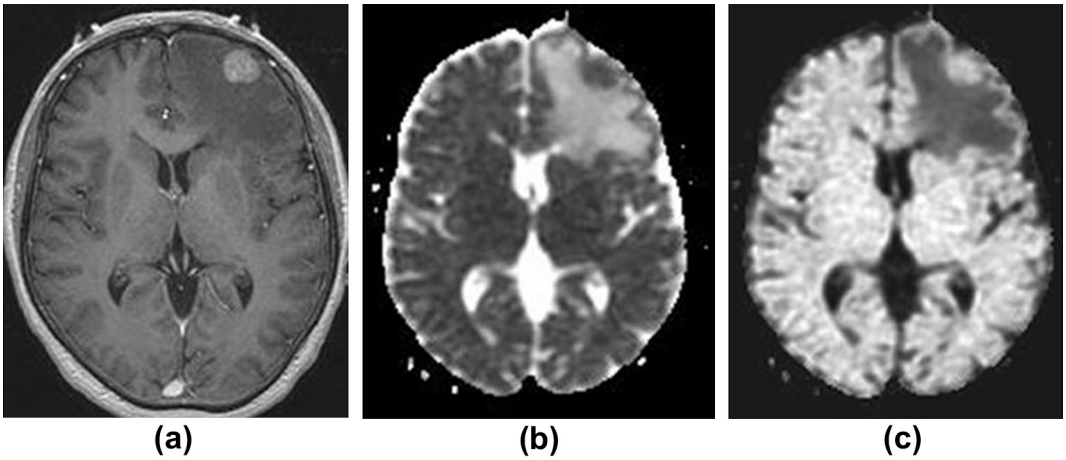

Figure 4 Histologically proven metastasis from lung cancer in a 60-year-old woman. (a) Contrast-enhanced T1-weighted image shows a nodular enhancing mass in the left frontal lobe with extensive peritumoural oedema. (b) On the ADC map, the ADC value is homogeneously elevated in the peritumoural region, thought to represent purely vasogenic oedema. (c) At exponential DWI, peritumoural oedema shows relatively homogeneous low signal intensity, which is thought to represent purely vasogenic oedema.

overall magnitude of diffusion, independent of tissue orientation, similar to the ADC. In the brain, FA, which is a measure of the directionality of molecular motion, is thought to reflect white matter fibre integrity.[26,27] FA in brain tumours has been found to be influenced by histological characteristics and correlates with cellularity, vascularity, cell density, neuronal and axonal structures, and fibre tracts.[28–30] Sinha et al.[28] explained the decrease in FA values within brain tumours as a loss of structural organization, whereas Beppu et al.[29] indicated that there is a positive correlation between FA values and both the cellularity and vascularity of tumours. However, there is still controversy, regarding the relationship between FA and tumour cellularity. In recent studies, a negative relationship was found when FA changes were correlated with cellularity, as determined histologically.[31,32]

DTI has been used previously in an attempt to differentiate between glioblastomas and cerebral metastases. Several investigators have tried to differentiate tumour-infiltrated oedema from purely vasogenic oedema.[2,27,33–35] Their results demonstrated significantly higher MD in the peritumoural oedema, which surrounds metastatic tumours when compared with that in the oedema surrounding high-grade gliomas. The marked peritumoural influx of water is probably secondary to greatly increased vascular permeability, which is presumably caused by the high expression of vascular endothelial growth factor, a trait that is common among metastatic lesions. Increases in the peritumoural MD for malignant gliomas are tempered by the infiltrative rather than expansile growth patterns with the presence of tumour cells in the peritumoural abnormality. Therefore, metastasis-related vasogenic oedema reflects a greater increase in water content of the surrounding tissue.[2,26,34] However, FA showed conflicting results when used to differentiate tumour-infiltrated oedema from purely vasogenic oedema. Several studies comparing metastasis with high-grade glioma reported that the peritumoural FA was not significantly different.[2,33,35] However, a few reports showed that FA was significantly lower within the oedema surrounding the metastases than within the oedema around glioblastomas.[36] Gupta et al.[26] demonstrated a reduced FA in the peritumoural region of malignant glioma. They emphasized that decreases in the peritumoural FA for malignant gliomas reflected the presence of infiltrating tumour cells, which may destroy rather than simply displace the white matter tracts.

As the oedematous region contains areas of increased extra- and intracellular water, tumour infiltration and the varying fractional composition of normal white–grey matter, it is difficult to determine which factor is reflected in FA metrics. The discrepancy between these studies may also be due to the difference in the selection of regions of interest (ROIs) in the peritumoural region. These might further explain the conflicting reports of FA characteristics in these regions.

Role of MR perfusion imaging

Dynamic susceptibility contrast perfusion imaging is based on the measurement of the MR signal intensity, using a T2*-weighted sequence, during the first pass of a bolus of a paramagnetic contrast agent. Tumour angiogenesis can be indirectly assessed using perfusion MRI-derived *in vivo* maps of the cerebral blood volume (CBV), which depict the overall tumour vascularity. Perfusion MRI measurements of relative CBV (rCBV) were calculated using the ratio between the CBV in the diseased area and in the contralateral white matter, and have been shown to correlate with both conventional angiographic assessments of tumour vascular density and histological measurements of tumour neovascularization. An increase in the microvascularity and neovascularity leads to increased rCBV ratios.[4,6,17,37]

Several studies in the literature have reported that tumoural rCBV ratios are not useful for discriminating metastatic tumours from high-grade gliomas.[19,21,38,39]

Perfusion MRI may be useful in differentiating a solitary metastasis from a primary glioma, based on the difference in the measurements of the peritumoural rCBV. The peritumoural regions of glioblastomas reveal an increase in the rCBV due to tumour infiltration and associated neoangiogenesis. This increase in the peritumoural rCBV may also reflect diffuse migration of glioma cells along vascular channels of the white matter tracts spreading beyond the visible tumour borders on the contrast-enhanced T1-weighted images (Fig 5). In contrast, in metastatic tumours, the peritumoural region represents the reaction of the surrounding intrinsically normal, but oedematous brain parenchyma.[37,40–45] Metastases spread via the blood flow and invade the capillary blood–brain barrier without inducing neoangiogenesis. Instead, metastases contain highly leaky capillaries within the contrast-enhancing area. Therefore, T2-weighted areas of hyperintensities seen in peritumoural regions surrounding metastases are likely to be vasogenic oedema associated with the leakiness of these abnormal capillaries. In addition, animal studies of cerebral perfusion have shown that blood flow in oedematous tissue is decreased due to a local compression of the microcirculation by extravasated fluid. These two factors may account for a decrease in rCBV in the peritumoural region of the metastases (Fig 6).[17,42,46,47]

Previous studies have shown that peritumoural rCBV was significantly lower in metastases than in glioblastoma.[4,6,17,37,40,45] Blasel et al.[45] showed that using the cut-off value 1 for discriminating metastases from GBM yielded a sensitivity of 96%, specificity of 64%, a PPV of 68% and a NPV of 95%.

Role of MRS

Proton MRS is a powerful, non-invasive imaging technique that offers unique metabolic information on brain tumour biology. Proton MRS captures the biochemical

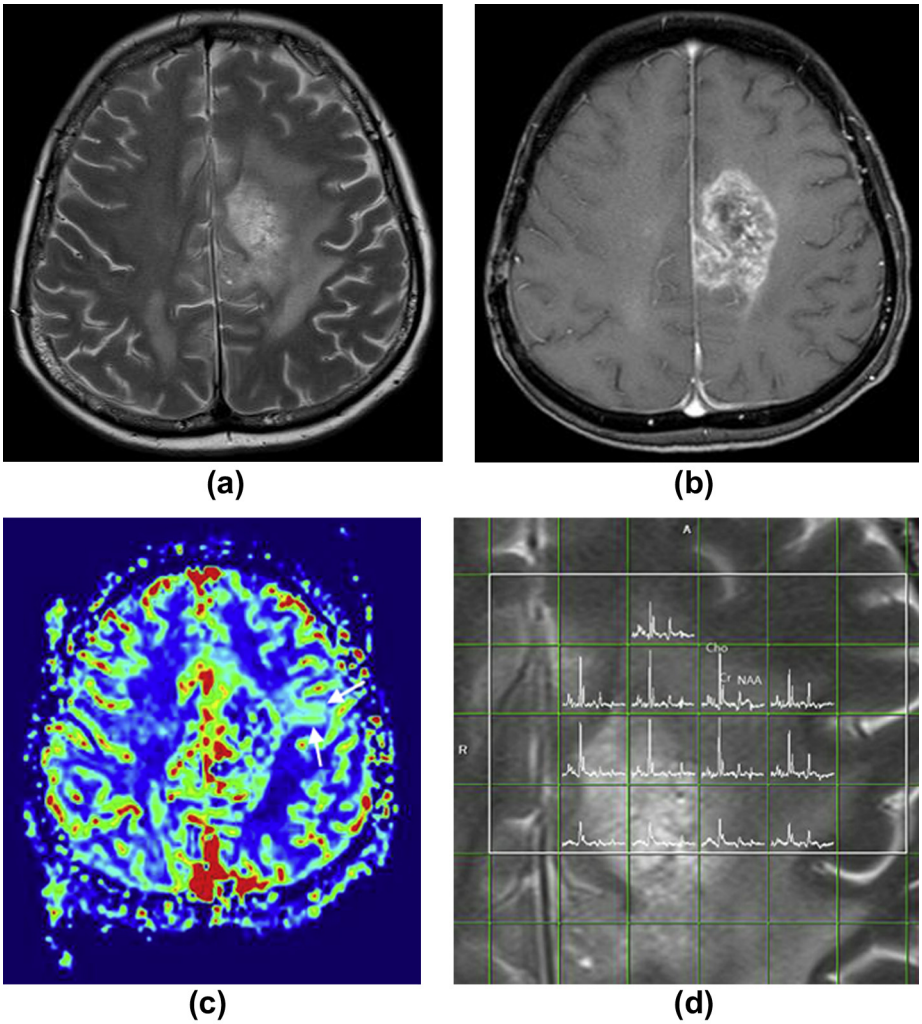

Figure 5 Histologically proven glioblastoma in a 60-year-old woman. (a) T2-weighted image and (b) contrast-enhanced T1-weighted image demonstrate a mass lesion showing heterogeneous enhancement with significant peritumoural oedema in the left parasagittal region. (c) Colour-coded rCBV perfusion image shows a large area with increased vascularity in the peritumoural region (arrows), as well as the left parasagittal enhancing mass. (d) Multivoxel MRS (echo time = 135 ms). Enhancing tumoural spectra show a markedly elevated Cho/Cr ratio. Peritumoural spectra also show an elevated Cho/Cr ratio, consistent with peritumoural tumour infiltration.

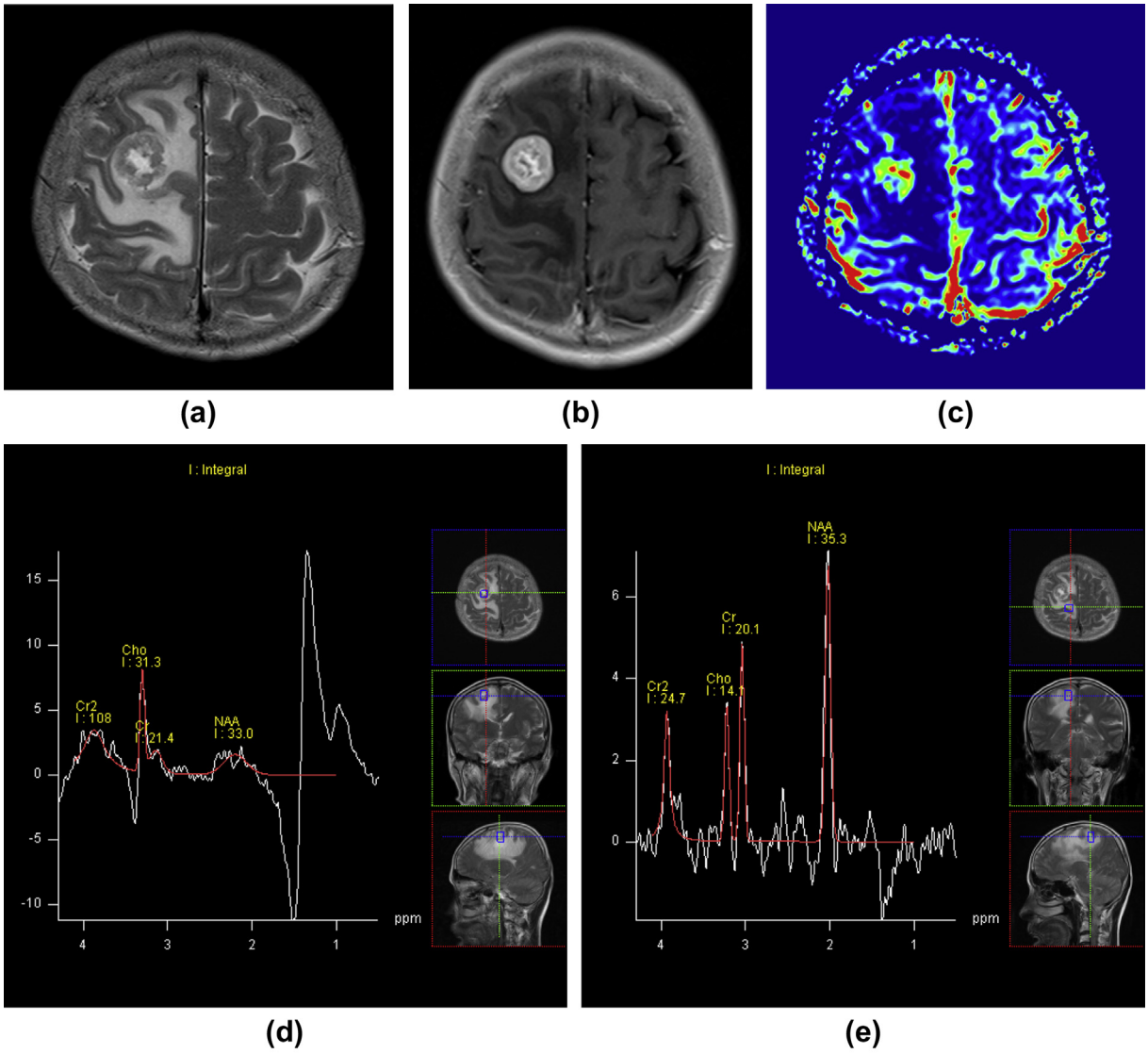

Figure 6 Histologically proven metastasis from breast cancer in a 61-year-old woman. (a) T2-weighted image and (b) contrast-enhanced T1-weighted image demonstrate a mass lesion showing intense contrast enhancement with significant peritumoural oedema in the right frontal lobe. (c) The colour-coded rCBV perfusion image shows tumoural hypervascularity with markedly decreased peritumoural vascularity. (d, e) Multivoxel MRS (echo time = 135 ms). (d) Enhancing tumoural spectrum shows markedly elevated Cho/Cr and decreased NAA/Cr ratios with markedly elevated lactate/lipid peak. (e) Peritumoural spectrum demonstrates no evidence of significant tumoural infiltration.

signature of normal and diseased brain tissue *in vivo*. The major brain metabolites detected by proton MRS are N-acetyl aspartate (NAA), choline (Cho), creatinine (Cr), myoinositol, lipid, lactate, glutamine, and glutamate. MRS allows for the differentiation of tumoural versus non-tumoural tissue, primarily through the differences in Cho metabolite. Cho is known to increase in the presence of increased cellular membrane turnover, and cellular proliferation; hence, it should be elevated in the areas of tumour infiltration, even in the absence of enhancement or T2 signal abnormality.[17,37,38]

The measurement of the intratumoural Cho/Cr ratio is not as useful as measuring the peritumoural Cho/Cr ratio to differentiate between glioblastomas and metastases. Most previous investigators have found no significant difference in the intratumoural spectra of metastases and high-grade gliomas,[4,48–53] although a few studies have suggested possible spectral differences between metastases and gliomas.[6,54] Previous studies have shown that an elevated Cho/Cr ratio was found in the peritumoural regions of glioblastomas, in keeping with tumoural infiltration (Fig 5d). No increase in the Cho/Cr ratio was found in the peritumoural region of metastasis (Fig 6d and e).[4,6,54,55]

NAA is a marker of neuronal integrity.[37] Law et al.[6] reported that there was no significant difference in the peritumoural NAA/Cr ratio between the two groups, because there is no neuronal replacement or destruction in the peritumoural regions of either condition. In glioblastoma, tumour cells infiltrate along vascular channels but do not destroy the pre-existing cyto-architecture. Vasogenic

oedema associated with metastases is also a passive process that does not necessarily destroy the underlying structure or neuronal tissue.[46,56]

Conclusion

Although the current neuroimaging standard for brain tumour diagnosis is conventional MRI, this technique alone is often unreliable for differentiating between glioblastoma and solitary metastatic lesions.[1–6] Advanced MRI methods are clinically applied to complement the morphological findings from anatomical MRI with metabolic and functional information. MRI is no longer just a research tool, and advanced MRI methods are rapidly becoming part of routine brain tumour imaging protocols to improve the diagnosis of intracranial mass lesions. Combined anatomical and physiological MRI promises more comprehensive tumour characterization and better understanding of tumour biology. Therefore, combined MRI techniques can substantially and non-invasively improve accuracy when differentiating between the tumour-infiltrating oedema associated with glioblastoma and the purely vasogenic oedema associated with metastasis.[37,50,57]

Although in large groups of patients differences in peritumoural oedema metrics between metastasis and glioblastoma can be found using advanced MRI techniques, in an individual patient these techniques may not be sufficiently sensitive or specific to prevent the need for invasive biopsy. Despite their potential for improving knowledge on brain tumour biology, advanced MRI methods still require additional validation.

References

1. Oh J, Cha S, Aiken AH, et al. Quantitative apparent diffusion coefficients and T2 relaxation times in characterizing contrast enhancing brain tumours and regions of peritumoral edema. *J Magn Reson Imaging* 2005; **21**:701–8.
2. Lu S, Ahn D, Johnson G, et al. Peritumoral diffusion tensor imaging of high-grade gliomas and metastatic brain tumors. *AJNR Am J Neuroradiol* 2003;**24**:937–41.
3. Tang YM, Ngai S, Stuckey S. The solitary enhancing cerebral lesion: can FLAIR aid the differentiation between glioma and metastasis? *AJNR Am J Neuroradiol* 2006;**27**:609–11.
4. Chiang IC, Kuo YT, Lu CY, et al. Distinction between high-grade gliomas and solitary metastases using peritumoral 3-T magnetic resonance spectroscopy, diffusion, and perfusion imagings. *Neuroradiology* 2004; **46**:619–27.
5. Bulakbasi N, Kocaoglu M, Ors F, et al. Combination of single-voxel proton MR spectroscopy and apparent diffusion coefficient calculation in the evaluation of common brain tumors. *AJNR Am J Neuroradiol* 2003;**24**:225–33.
6. Law M, Cha S, Knopp EA, et al. High-grade gliomas and solitary metastases: differentiation by using perfusion and proton spectroscopic MR imaging. *Radiology* 2002;**222**:715–21.
7. Maurer MH, Synowitz M, Badakshi H, et al. Glioblastoma multiforme versus solitary supratentorial brain metastasis: differentiation based on morphology and magnetic resonance signal characteristics. *Rofo* 2013; **185**:235–40.
8. Giese A, Westphal M. Treatment of malignant glioma: a problem beyond the margins of resection. *J Cancer Res Clin Oncol* 2001;**127**:217–25.
9. Soffietti R, Ruda R, Mutani R. Management of brain metastases. *J Neurol* 2002;**249**:1357–69.
10. Stuckey SL, Wijedeera R. Multicentric/multifocal cerebral lesions: can fluid-attenuated inversion recovery aid the differentiation between glioma and metastases? *J Med Imaging Radiat Oncol* 2008;**52**:134–9.
11. Pavlisa G, Rados M, Pavilisa G, et al. The difference of water diffusion between brain tissue infiltrated by tumor and peritumoral vasogenic edema. *Clin Imaging* 2009;**33**:96–101.
12. Yamasaki F, Kurisu K, Satoh K, et al. 231 Apparent diffusion coefficient of human brain 232 tumors at MR imaging. *Radiology* 2005;**235**:985–91.
13. Kono K, Inoue Y, Nakayama K, et al. The role of diffusion-weighted imaging in patients with brain tumors. *AJNR Am J Neuroradiol* 2001; **22**:1081–8.
14. Krabbe K, Gideon P, Wagn P, et al. MR diffusion imaging of human intracranial tumors. *Neuroradiology* 1997;**39**:483–9.
15. Sugahara T, Korogi Y, Kochi M, et al. Usefulness of diffusion-weighted MRI with echo-planar technique in the evaluation of cellularity in gliomas. *J Magn Reson Imaging* 1999;**9**:53–60.
16. Kitis O, Altay H, Calli C, et al. Minimum apparent diffusion coefficients in the evaluation of brain tumors. *Eur J Radiol* 2005;**55**:393–400.
17. Cha S. Update on brain tumor imaging: from anatomy to physiology. *AJNR Am J Neuroradiol* 2006;**27**:475–87.
18. Calli C, Kitis O, Yunten N, et al. Perfusion and diffusion MR imaging in enhancing malignant cerebral tumors. *Eur J Radiol* 2006;**58**:394–403.
19. Stadnik TW, Chaskis C, Michotte A, et al. Diffusion-weighted MR imaging of intracerebral masses: comparison with conventional MR imaging and histologic findings. *AJNR Am J Neuroradiol* 2001;**22**:969–76.
20. Rollin N, Guyotat J, Streichenberger N, et al. Clinical relevance of diffusion and perfusion magnetic resonance imaging in assessing intra-axial brain tumors. *Neuroradiology* 2006;**48**:150–9.
21. Lee EJ, terBrugge K, Mikulis D, et al. Diagnostic value of peritumoral minimum apparent diffusion coefficient for differentiation of glioblastoma multiforme from solitary metastatic lesions. *AJR Am J Roentgenol* 2011;**196**:71–6.
22. Server A, Kulle B, Maehlen J, et al. Quantitative apparent diffusion coefficients in the characterization of brain tumors and associated peritumoral edema. *Acta Radiol* 2009;**50**:682–9.
23. van Westen D, Lätt J, Englund E, et al. Tumor extension in high grade gliomas assessed with diffusion magnetic resonance imaging: values and lesion-to-brain ratios of apparent diffusion coefficient and fractional anisotropy. *Acta Radiol* 2006;**47**:311–9.
24. Provenzale JM, Engelter ST, Petrella JR, et al. Use of MR exponential diffusion-weighted images to eradicate T2 “shine-through” effect. *AJR Am J Roentgenol* 1999;**172**:537–9.
25. Hakyemerz B, Aksoy U, Yildiz H, et al. Intracranial epidermoid cysts: diffusion weighted, FLAIR and conventional MR findings. *Eur J Radiol* 2005;**54**:214–20.
26. Gupta A, Shah A, Young RJ, et al. Imaging of brain tumors: functional magnetic resonance imaging and diffusion tensor imaging. *Neuroimaging Clin N Am* 2010;**20**:379–400.
27. Byrnes TJ, Barrick TR, Bell BA, et al. Diffusion tensor imaging discriminates between glioblastoma and cerebral metastases *in vivo*. *NMR Biomed* 2011;**24**:54–60.
28. Sinha S, Bastin ME, Wittle IR, et al. Diffusion tensor MR imaging of high-grade cerebral gliomas. *AJNR Am J Neuroradiol* 2002;**23**:520–7.
29. Beppu T, Inoue T, Shibata Y, et al. Measurement of fractional anisotropy using diffusion tensor MRI in supratentorial astrocytic tumors. *J Neurooncol* 2003;**6**:109–16.
30. White ML, Zhang Y, Yu F, et al. Diffusion tensor MR imaging of cerebral gliomas: evaluation fractional anisotropy characteristics. *AJNR Am J Neuroradiol* 2011;**32**:374–81.
31. Toh CH, Castillo M, Wong AM, et al. Primary cerebral lymphoma and glioblastoma multiforme: differences in diffusion characteristics evaluated with diffusion tensor imaging. *AJNR Am J Neuroradiol* 2008;**29**:471–5.
32. Stadlbauer A, Ganslandt O, Buslei R, et al. Gliomas: histopathologic evaluation of changes in directionality and magnitude of water diffusion at diffusion-tensor MR imaging. *Radiology* 2006;**240**:803–10.
33. Wang W, Steward CE, Desmond PM. Diffusion tensor imaging in glioblastoma multiforme and brain metastases: the role of p, q, L and fractional anisotropy. *AJNR Am J Neuroradiol* 2009;**30**:203–8.
34. Lu S, Ahn D, Johnson G, et al. Diffusion tensor MR imaging of intracranial neoplasia and associated peritumoral edema: introduction of the tumor infiltration index. *Radiology* 2004;**232**:221–8.

35. Tsuchiya K, Fujikawa A, Nakajima M, et al. Differentiation between solitary brain metastasis and high-grade glioma by diffusion tensor imaging. *Br J Radiol* 2005;**78**:533–7.
36. Wang S, Kim S, Chawla S, et al. Differentiation between glioblastomas and solitary brain metastases using diffusion tensor imaging. *Neuroimage* 2009;**44**:653–60.
37. Cha S. Neuroimaging in neuro-oncology. *Neurotherapeutics* 2009;**6**: 465–77.
38. Cho SK, Na DG, Ryoo JW, et al. Perfusion MR imaging: clinical utility for the differential diagnosis of various brain tumors. *Korean J Radiol* 2002; **3**:171–9.
39. Kremer S, Grand S, Remy C, et al. Cerebral blood volume mapping by MR imaging in the initial evaluation of brain tumors. *J Neuroradiol* 2002; **29**:105–13.
40. Hakyemez B, Erdogan C, Bolca N, et al. Evaluation of different cerebral mass lesions by perfusion-weighted MR imaging. *J Magn Reson Imaging* 2006;**24**:817–24.
41. Machein MR, Plate KH. VEGF in brain tumors. *J Neurooncol* 2000; **50**:109–20.
42. Cha S, Knopp EA, Johnson G, et al. Intracranial mass lesions: dynamic contrast-enhanced susceptibility-weighted echo-planar perfusion MR imaging. *Radiology* 2002;**223**:11–29.
43. Blasel S, Franz K, Mittelbronn M, et al. The striate sign: peritumoural perfusion pattern of infiltrative primary and recurrent gliomas. *Neurosurg Rev* 2010;**33**:193–204.
44. Claes A, Idema AJ, Wesseling P. Diffuse glioma growth: a guerrilla war. *Acta Neuropathol* 2007;**114**:443–58.
45. Blasel S, Jurcoane A, Franz K, et al. Elevated peritumoural rCBV values as a mean to differentiate metastases from high-grade gliomas. *Acta Neurochir (Wien)* 2010;**152**:1893–9.
46. Zhang M, Olsson Y. Hematogenous metastases of the human brain—characteristics of peritumoral brain changes: a review. *J Neurooncol* 1997;**35**:81–9.
47. Server A, Orheim TE, Graff BA, et al. Diagnostic examination performance by using microvascular leakage, cerebral blood volume, and blood flow derived from 3-T dynamic susceptibility-weighted contrast-enhanced perfusion MR imaging in the differentiation of glioblastoma multiforme and brain metastasis. *Neuroradiology* 2011;**53**:319–30.
48. McBride DQ, Miller BL, Nikas DL, et al. Analysis of brain tumors using 1H magnetic resonance spectroscopy. *Surg Neurol* 1995;**44**:137–44.
49. Bruhn H, Frahm J, Gyngell ML, et al. Noninvasive differentiation of tumors with use of localized H-1 MR spectroscopy *in vivo*: initial experience 299 in patients with cerebral tumors. *Radiology* 1989;**172**:541–8.
50. Al-Okaili RN, Krejza J, Wang S, et al. Advanced MR imaging techniques in the diagnosis of intraaxial brain tumors in adults. *RadioGraphics* 2006; **26**:S173–89.
51. Sijens PE, Knopp MV, Brunetti A, et al. 1H MR spectroscopy in patients with metastatic brain tumors: a multicenter study. *Magn Reson Med* 1995;**33**:818–26.
52. Poptani H, Gupta RK, Roy R, et al. Characterization of intracranial mass lesions with *in vivo* proton MR spectroscopy. *AJNR Am J Neuroradiol* 1995;**16**:1593–603.
53. Fulham MJ, Bissi A, Dietz MJ, et al. Mapping of brain tumor metabolites with proton MR spectroscopic imaging: clinical relevance. *Radiology* 1992;**185**:675–86.
54. Fan G, Sun B, Wu Z, et al. *In vivo* single-voxel proton MR spectroscopy in the differentiation of high-grade gliomas and solitary metastases. *Clin Radiol* 2004;**59**:77–85.
55. Server A, Josefsen R, Kulle B, et al. Proton magnetic resonance spectroscopy in the distinction of high-grade cerebral gliomas from single metastatic brain tumors. *Acta Radiol* 2010;**51**:316–25.
56. Knopp EA, Cha S, Johnson G, et al. Glial neoplasms: dynamic contrast-enhanced T2*-weighted MR imaging. *Radiology* 1999;**211**:791–8.
57. Al-Okaili RN, Krejza J, Woo JH, et al. Intraaxial brain masses: MR imaging-based diagnostic strategy—initial experience. *Radiology* 2007; **243**:539–50.